

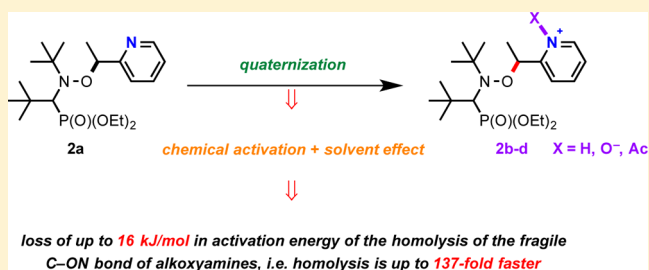
Chemically Triggered C–ON Bond Homolysis of Alkoxyamines. 8. Quaternization and Steric Effects

G rard Audran, Lionel Bosco, Paul Br mond,* Sylvain R. A. Marque,* Val rie Roubaud, and Didier Siri

Aix-Marseille Universit , CNRS, Institut de Chimie Radicalaire UMR 7273, Avenue Escadrille Normandie-Niemen, 13397 Marseille cedex 20, France

S Supporting Information

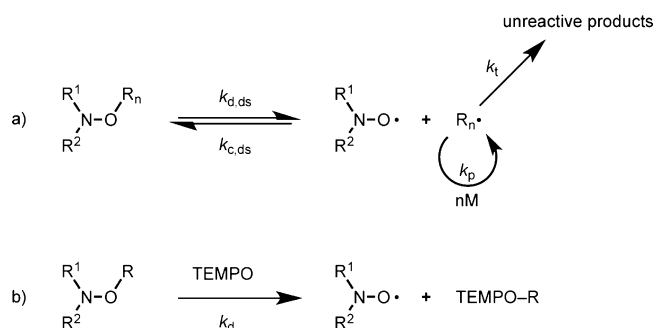
ABSTRACT: The C–ON bond homolysis in alkoxyamine **2a** was chemically triggered by quaternization of the 1-(pyridin-2-yl)ethyl fragment using protonation, acylation, and oxidation into the *N*-oxide. The solvent effect was also investigated, and DFT calculations were performed to explore this chemical activation. Alkoxyamines **2a–d** were also compared to the 1-(pyridin-4-yl)ethyl analogues **3a–d**.



INTRODUCTION

For more than two decades, extensive efforts from academic and industrial laboratories have been devoted to the development of nitroxide-mediated polymerization (NMP), in which nitroxide/alkoxyamine couples are used as controller/initiator reagents, respectively.^{1–6} NMP is summarized in a three-stage polymerization process (Scheme 1a) using the following kinetic

Scheme 1. (a) Simplified Scheme for NMP; (b) Conditions for Investigation of the C–ON Bond Homolysis in **2a–g**



parameters: $k_{d,ds}$, the rate constant of the homolysis of the C–ON bond of the dormant species (ds) to give nitroxyl and macroalkyl radicals; $k_{c,ds}$, the rate constant of the cross-coupling reaction between nitroxyl and alkyl radicals; k_p , the propagation rate constant; and k_t , the termination rate constant. The main advantage of NMP is the quasi-absence of termination reactions due to the low concentration of active species and to the equilibrium between the dormant and active species. It is now clear that the success of NMP depends on precise tuning of the homolysis rate constant k_d and the re-formation rate constant k_c for the initiating alkoxyamine as well as $k_{d,ds}$ and $k_{c,ds}$ for the

dormant species.^{1,2,7} This has led several groups to develop alkoxyamines suitable only for a few monomers: for example, alkoxyamine **1** (Figure 1) is efficient in triggering and

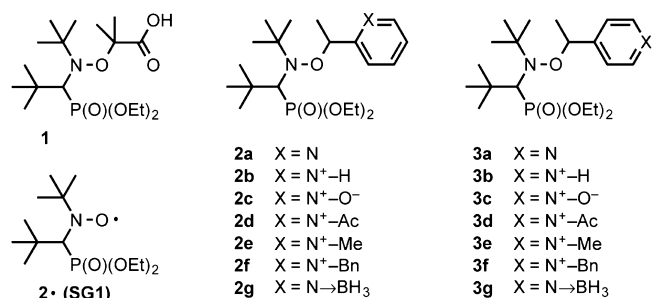


Figure 1. Structures of activated alkoxyamines and SG1 nitroxide.

controlling the NMP of monosubstituted monomers (e.g., styrenic and alkyl acrylate monomers) but unsuccessful for 1,1-disubstituted monomers (e.g., cumenic and alkyl methacrylate monomers) under general conditions.⁸ Beyond these facts, new strict conditions have emerged about the shipping of low-temperature-labile materials.⁹ Therefore, the development of chemically triggered C–ON bond homolysis is an active field for NMP improvement.

The puzzling results of Mazarin et al.¹⁰ were recently confirmed by Bagryanskaya and co-workers, who showed that protonation of the nitroxide part of an alkoxyamine induces a decrease in k_d .¹¹ At the same time, we reported that protonation of the pyridine-containing alkyl part of **3a** to afford **3b** led to a striking increase in k_d .^{12,13} We then investigated the effects of the oxidation (**3c**), quaternization (**3d–f**), and complexation with a Lewis acid (**3g**) of the

Received: August 7, 2013

Published: September 23, 2013

Scheme 2. Preparation of Alkoxyamines 2a–d and 2g

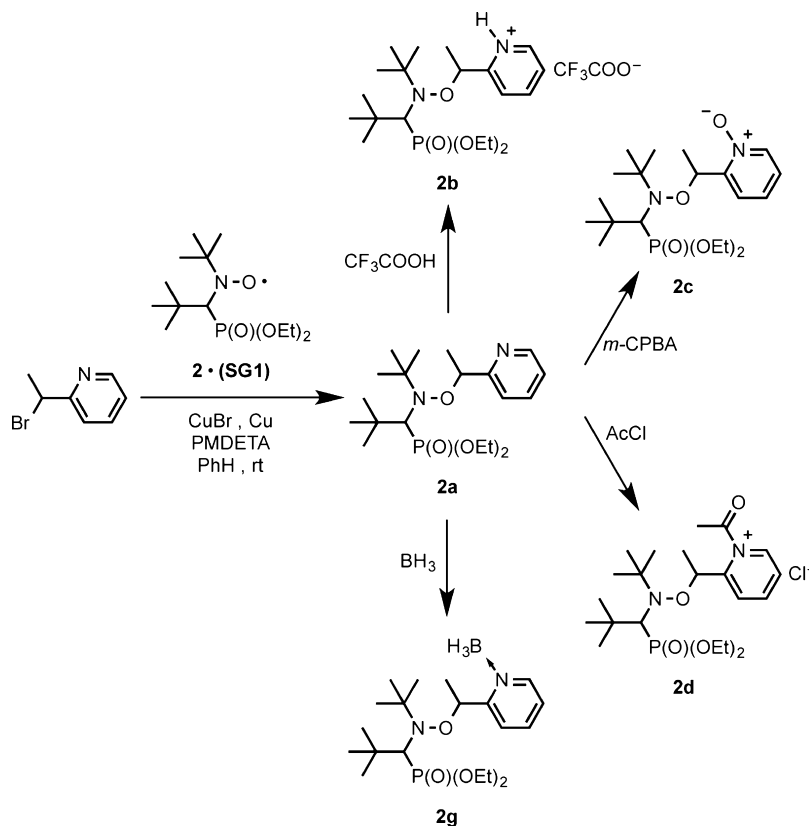


Table 1. Experimental Temperatures T ($^{\circ}\text{C}$), C–ON Bond Homolysis Rate Constants k_d , Activation Energies E_a , Re-estimated k_d' Values at 120°C , and Relative Rate Constants $k_{d,\text{rel}}$ ^a for the Minor and Major Diastereoisomers of Alkoxyamines 2a–d and 3a–d

T ($^{\circ}\text{C}$)	k_d (10^{-4} s^{-1}) ^{b,c}		E_a (kJ/mol) ^d		k_d' (10^{-2} s^{-1}) ^e		$k_{d,\text{rel}}$ (120 $^{\circ}\text{C}$)		E_a (kJ/mol) ^f		k_d' (10^{-2} s^{-1}) ^f		$k_{d,\text{rel}}$ (120 $^{\circ}\text{C}$) ^f			
	minor ^g	major ^g	minor ^g	major ^g	minor ^g	major ^g	minor ^g	major ^g	minor ^h	major ^h	minor ^h	major ^h	minor ^h	major ^h		
2a	80	1.07	1.17	124.1	123.8	0.79	0.85	1	1	3a	123.0	123.0	1.00	0.92	1	1
2a' ⁱ	80	2.62	1.82	121.4	122.5	1.76	1.27	2.2	1.5	3a' ⁱ	119.2	119.4	3.48	3.32	3.5	3.6
2b	61	1.77	1.62	116.0	116.2	9.31	8.64	11.8	10.2	3b	115.6	115.7	11.2	7.63	11.2	8.3
2b' ⁱ	60	28.3	19.7	108.0	109.0	108	79.8	136.7	93.9	3b' ⁱ	108.9	109.7	80.9	63.3	80.9	68.8
2c	60	1.57	3.05	116.0	114.1	9.36	16.4	11.8	19.2	3c	113.9	113.7	17.4	19.0	17.4	20.7
2c' ⁱ	61	1.38	2.31	116.7	115.3	7.54	11.7	9.5	13.8	3c' ⁱ	111.8	111.7	33.2	34.4	33.2	37.4
2d	61	0.65	0.75	118.8	118.4	3.97	4.92	5.0	5.8	3d	114.8	115.4	13.4	11.0	13.4	12.0

^a $k_{d,\text{rel}} = k_{d,2a-d} / k_{d,2a}$ or $k_{d,3a-d} / k_{d,3a}$. ^bThis work. Measurements were performed in *t*-BuPh as the solvent unless otherwise mentioned. ^cMeasured at the temperature reported in the second column. In general, the reported values are averages of two runs. The statistical error is less than 2%. For all of the reported values, the error is lower than 5% and is mainly due to discrepancies in the temperature measurements. ^dActivation energies E_a estimated by applying the averaged frequency factor $A = 2.4 \times 10^{14} \text{ s}^{-1}$ (see ref 19). Error was given as less than 2 kJ/mol. ^e k_d' values re-estimated at 120°C using the E_a values given in the fifth and sixth columns and $A = 2.4 \times 10^{14} \text{ s}^{-1}$. ^fData from refs 14, 15, and 21. ^gFor a tentative attribution, see ref 22. ^hThe minor diastereoisomer is the *SS/RR* one, and the major diastereoisomer is the *SR/RS* one (see ref 12). ⁱIn 1:1 (v/v) MeOH/H₂O as the solvent.

pyridinyl fragment.¹⁴ The results were astonishing, as up to 200-fold increases in k_d were measured.¹⁴ These activations were also investigated by DFT calculations, and we very recently reported the solvent effect on the activated alkoxyamines 3a, 3c, and 3e by screening of 15 solvents.^{15,16} Alkoxyamines 3a and 3b were also tested on benchmark NMP systems and performed as well as alkoxyamine 1.¹³ Having extensively studied the kinetic aspects of alkoxyamine 3a and its chemically activated derivatives 3b–g, we then turned our attention toward alkoxyamine 2a and its corresponding derivatives 2b–g in order to determine the influence of the steric effect on the activation by changing the alkyl part from 1-

(pyridin-4-yl)ethyl radical to 1-(pyridin-2-yl)ethyl radical. DFT calculations on these new alkoxyamines were also performed.

RESULTS AND DISCUSSION

Alkoxyamine 2a was prepared from the nitroxide *N*-(2-methylpropyl)-*N*-(1-diethylphosphono-2,2-dimethylpropyl)-*N*-oxyl (SG1) and 2-(1-bromoethyl)pyridine using Matyjaszewski's procedure,¹⁷ which afforded 2a as a 2:1 mixture of diastereoisomers (Scheme 2; also see the Supporting Information). Alkoxyamines 2b–d and 2g were then synthesized from the mother compound 2a using trifluoroacetic

acid (**2b**), *m*-chloroperoxybenzoic acid (**2c**), acetyl chloride (**2d**), and borane–THF complex (**2g**). Compounds **2b** and **2d** were prepared in situ, and compounds **2c** and **2g** were prepared in quantitative yields and purified by precipitation or solvent removal in vacuo. Each compound was thus obtained as a 2:1 mixture of diastereoisomers. Attempts to prepare **2e** and **2f** by methylation and benzylation, respectively, under different conditions did not afford the corresponding quaternized alkoxyamines, presumably because of an important steric hindrance around the nitrogen of the pyridinyl ring, leading to a decrease in its reactivity.

Rate constants were measured as previously described using 2 equiv of TEMPO as an alkyl radical scavenger in *tert*-butylbenzene (*t*-BuPh) as the solvent (Scheme 1b).¹⁸ Except for **2b** and **2d**, which were generated in situ, all of the other k_d values were measured using pure compounds (Table 1). Figure 2 displays the plots for the first-order decays of the activated

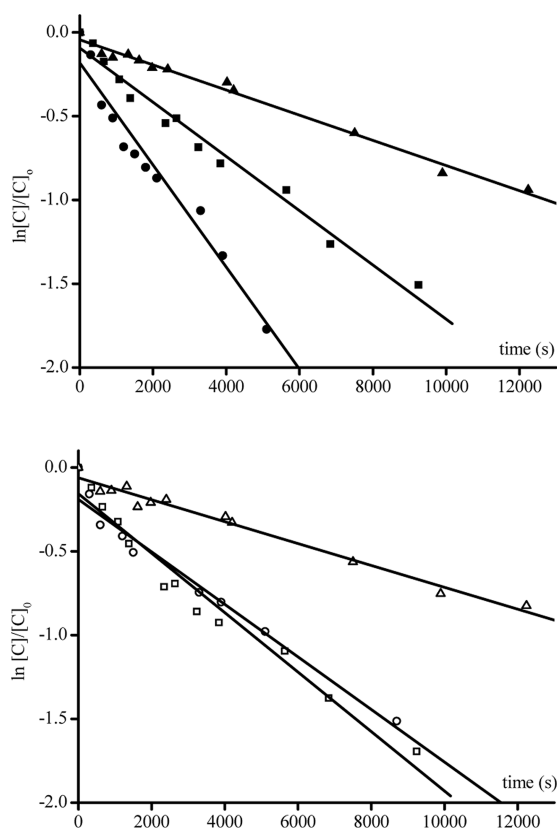


Figure 2. Plots of $\ln([alkoxyamine]_t/[alkoxyamine]_{t=0})$ vs t for the major (top) and minor (bottom) diastereoisomers of **2b** (■, □), **2c** (●, ○), and **2d** (▲, △) at 60 °C in *t*-BuPh.

major and minor diastereoisomers of alkoxyamines **2b–d**. The activation energies E_a (Table 1) were estimated using the averaged frequency factor $A = 2.4 \times 10^{14} \text{ s}^{-1}$.^{19,20}

Upon heating, alkoxyamine **2g** afforded several compounds (as determined by ³¹P NMR spectroscopy) that did not decay in the same way. However, the sum of all the compounds afforded a k_d value very close to those reported for **2a**. Thus, different compounds might be observed because of the existence of rotamers. Furthermore, the dative bond of amine–borane **2g** might have been cleaved upon heating to release **2a**, and consequently, the measured k_d may have been the one for **2a** and not that for **2g**.²³

From the values measured for **2b–d**, it was clear that chemical activation of **2a** was still possible, with a 5- to 20-fold increase in k_d , despite the increase in steric hindrance around the nitrogen atom. The corresponding drop in E_a through chemical activation was 8–10 kJ/mol. For alkoxyamines **3b–g**, we previously observed different k_d values for the diastereoisomers.^{14–16} In contrast, similar k_d values were measured for both diastereoisomers of alkoxyamines **2a**, **2b**, and **2d**. The efficiency of the activation depends on the type of activation, that is, $k_{d,2b} \approx k_{d,2c} \approx 2.3 \times k_{d,2d} \approx 12 \times k_{d,2a}$ for the minor diastereoisomers and $k_{d,2b} \approx 1.8 \times k_{d,2d} \approx 10 \times k_{d,2a}$ for the major diastereoisomers. One should also notice that the homolysis of the major diastereoisomer of **2c** is ca. 1.7-fold faster than that of the minor diastereoisomer, leading to a 19-fold increase in k_d relative to **2a** (vide infra).

However, it must be stressed that the k_d values for **2a** after protonation (i.e., for **2b**) are very close to those for **3b**, meaning that the same effects are involved (Table 1 and vide infra).

Indeed, we very recently showed that the increase in k_d under activation is due to the increase in the electronegativity (χ) on the carbon atom of the C–ON bond, which results in weakening of the C–ON bond, as given by eq 1,^{24,25} which links the bond dissociation energy (BDE) to the square of the difference between the electronegativities of the atoms forming the bond and shows that a smaller electronegativity difference leads to a weaker bond.¹⁴

$$\text{BDE}_{(A-B)} = \frac{1}{2} [\text{BDE}_{(A-A)} + \text{BDE}_{(B-B)}] + 96.23(\chi_A - \chi_B)^2 \quad (1)$$

Moreover, we showed that for *t*-BuPh as the solvent, intimate ion pairs are expected, and therefore, the positive charge is partly used to neutralize the negative charge maintained in a close neighborhood, weakening the polar effect. In contrast, in a more polar solvent, the charge dissociation is expected to be more effective, leading to a stronger effect of the positive charge in increasing χ of the carbon atom of the C–ON bond and consequently to an increase in k_d .^{15,16,21}

The pD dependence of the ¹H NMR chemical shifts for **2a** and **2b** (Scheme 3) was investigated at room temperature in 1:1 (v/v) MeOH-*d*₄/D₂O, as alkoxyamine **2a** is not soluble in water. From pD 1.0 to 8.5, significant shifts were observed for the aromatic protons of the major and minor diastereoisomers from 8.65 and 8.60 to 7.90 and 7.85 ppm, respectively (Figure 3). The titration curve for the diastereoisomers of **2a** (Scheme 3) could be described by the Henderson–Hasselbach equation²⁶ (eq 2) and afforded pK_a values of 4.21 and 3.99 for the major and minor diastereoisomers of **2a**, respectively; these are at least 1.6 pK_a unit lower than the pK_a value for the corresponding 2-ethylpyridine (pK_a = 5.89)²⁷ because of the presence of the nitroxyl fragment, which acts as an electron-withdrawing group.

$$\delta_{\text{pD}} = \delta_{2a} + \frac{\delta_{2b} - \delta_{2a}}{1 + 10^{\text{pK}_a - \text{pD}}} \quad (2)$$

The pH dependence of k_d was therefore investigated at pH 7.0, where **2a** is the major species (>99%), and at pH 2.5, where **2b** is the major species (>99%). When the homolysis rate constants for **2a** and **2b** were measured in 1:1 (v/v) MeOH/H₂O as the solvent, a small 2-fold increase in k_d was observed for **2a** and a clear 10-fold increase in k_d was observed for **2b**

Scheme 3. Titration Curves for the Major (◆) and Minor (◇) Diastereoisomers of **2a** Obtained Using ^1H NMR Chemical Shifts in the Aromatic Zone of **2a** (0.02 M) at Room Temperature in 1:1 (v/v) MeOH- d_4 /D $_2$ O (pD Was Set with DCl and NaOD)

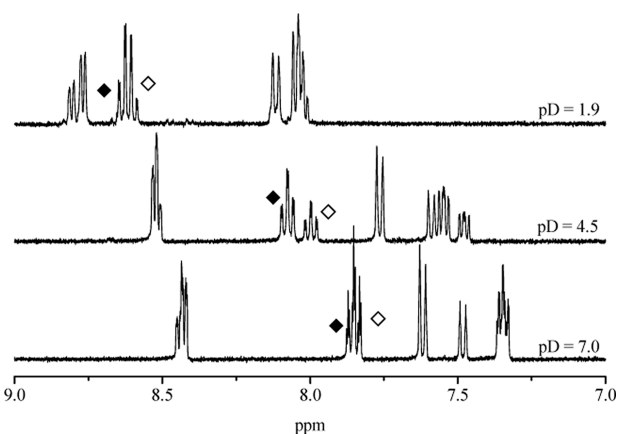
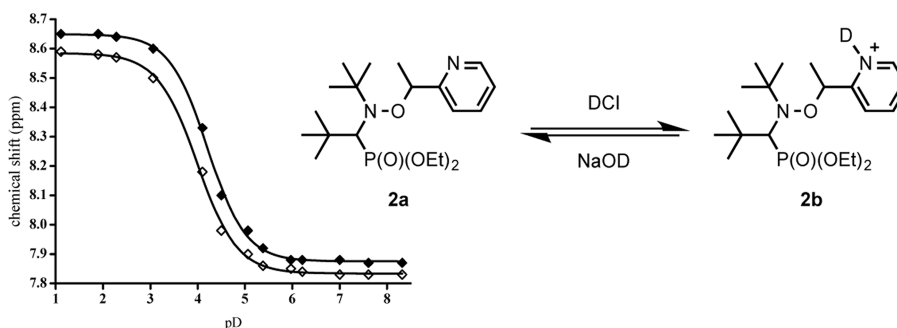


Figure 3. Aromatic zone of the ^1H NMR spectra of a 2:1 mixture of the major (◆) and minor (◇) diastereoisomers of **2a** (0.02 M) at pD = 1.9 (top), 4.5 (middle), and 7.0 (bottom) at room temperature in 1:1 (v/v) MeOH- d_4 /D $_2$ O. pD was set with DCl and NaOD. When the NMR signals of the diastereoisomers overlapped, they were ascribed using coupling constants.

relative to the k_d measured in *t*-BuPh, in good agreement with the data reported for alkoxyamines **3a** and **3b**.¹³ Consequently, activation by protonation led to a 62-fold increase in k_d when it occurred in MeOH/H $_2$ O, while it resulted in only an 11-fold increase in *t*-BuPh. When the solvent and the activation effects were combined, a 94- to 137-fold increase in k_d was observed, depending on the diastereoisomer. Alkoxyamine **2b** seemed to experience stronger solvent and activation effects than alkoxyamine **3b**, where these effects led to a 8-fold increase for the solvent effect, a 22-fold increase for the activation effect, and a 69- to 81-fold increase in k_d when these effects were combined, depending on the diastereoisomer. In fact, the averaged activation energies of the diastereoisomers of **2b** are very close to those of **3b** in *t*-BuPh ($\Delta E_a = 0.5$ kJ/mol) and in MeOH/H $_2$ O ($\Delta E_a = 0.8$ kJ/mol), while the activation energies of **2a** and **3a** are more different in *t*-BuPh ($\Delta E_a = 1.0$ kJ/mol) and in MeOH/H $_2$ O ($\Delta E_a = 2.7$ kJ/mol). This led us to assume that the solvent effect on **2a** is greater than that on **2b**. While it is clear that the nitrogen atom is more congested in **2a** than in **3a** and therefore is less accessible to the solvent, it is rather uncertain on which state (reactant, products, transition state) this solvent effect occurs on **2a**. The same comments hold for **2c**.

To gain deeper insight into the various effects involved in the chemical activation of the C–ON bond homolysis in alkoxyamines, calculations were performed using the B3LYP/

6-31G(d,p) method to optimize the geometries and to determine natural bond orbital (NBO) charges for **2a–c** in toluene. For the sake of simplicity, calculations were performed only on the RR/SS diastereoisomer, and they showed that alkoxyamines **2a–c** display similar values for the geometric parameters of the reactive center ($l_{\text{O1–C13}}$, $l_{\text{N2–O1}}$, $d_{\text{N2...C13}}$, and α_{N2O1C13} ; Table 1SI in the Supporting Information), meaning that quaternization of the nitrogen atom of the pyridinyl ring did not give rise to any significant structural changes. Thus, as already reported,^{28,29} the differences in $k_{d,2a}$, $k_{d,2b}$, and $k_{d,2c}$ could not be correlated with the geometric parameters of the reactive center.

The calculated Gibbs energies for the homolysis were in good agreement with the observed reactivities: $\Delta_r G$ in toluene decreased in going from **2a** to **2b** ($\Delta\Delta_r G = -2.5$ kJ/mol) and from **2a** to **2c** ($\Delta\Delta_r G = -16.4$ kJ/mol) as k_d increased. To probe the polar effect, the NBO atomic charges on the aromatic moiety were calculated (Figure 4 top). As expected from the

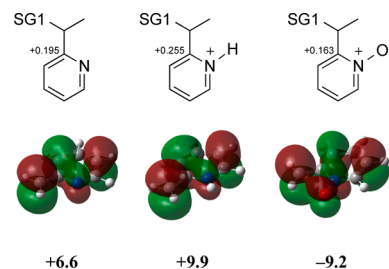
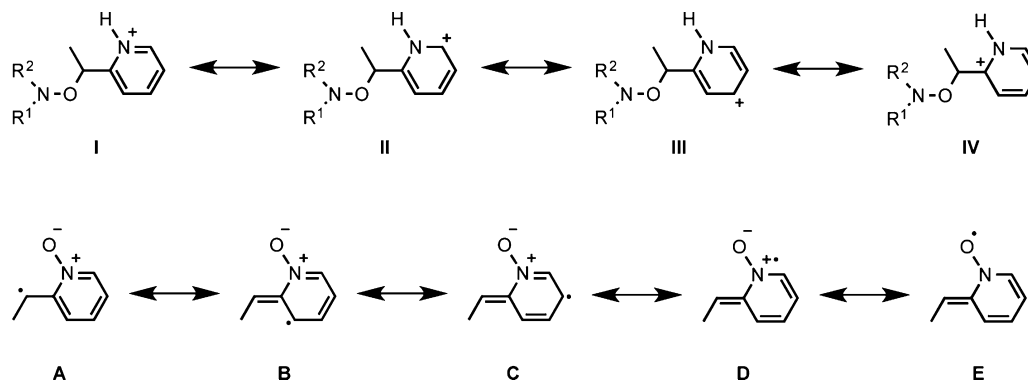


Figure 4. UB3LYP/6-31G(d,p) NBO charges (top) for **2a–c** (left to right, respectively) and UBMK/6-311+G(3df,2p)//RB3LYP/6-31G(d) SOMOs (middle) and RSEs (kJ/mol, bottom) of the corresponding benzylic radical models *ortho-a*•, *ortho-b*• and *ortho-c*• (left to right, respectively).

mesomeric forms I–IV (Scheme 4 top), protonation of **2a** to afford **2b** implied positive partial charges located at the *ipso* position (Figure 4 top) whereas a significant decrease in the charge at the *ipso* position was observed for **2c**. These changes in partial NBO charges are related to the changes in the electronegativity of the carbon atom in the C–ON bond. An increase in the partial charge at the *ipso* position involves an increase in χ for the carbon atom, which leads to a lower BDE (see eq 1) and consequently an increase in k_d , in nice agreement with the results observed for **2a** and **2b**. However, the lower partial charge at the *ipso* position for **2c** than **2a** would imply a larger k_d value for **2a** than for **2c**, in sharp contrast with the results reported (Table 1). This confirmed

Scheme 4. Mesomeric Forms of 2b (top) and *ortho-c*• (bottom)

that the polar effect is similarly involved for *ortho* (2a–g) and *para* (3a–g) pyridinyl-based alkoxyamines and does not account for all of the effects involving the reactions observed, highlighted by $k_{d,2c} = k_{d,2b}$ for the minor diastereoisomer and $k_{d,2c} \approx 2 \times k_{d,2b}$ for the major diastereoisomer whereas $k_{d,3c} \approx 2 \times k_{d,3b}$ for both diastereoisomers.

To probe the stabilization of the released alkyl radical, the radical stabilization energies (RSEs) of the benzylic radical models (*ortho-a*•, *ortho-b*•, and *ortho-c*•; Figure 4 bottom) were calculated with the UBMK/6-311+G(3df,2p)//RB3LYP/6-31G(d) method.³⁰ The positive RSEs of the benzylic radical models *ortho-a*• and *ortho-b*• (Figure 4 bottom) showed that the presence of either a heteroatom in the aromatic ring or a charge implies a destabilization of the released radical, whereas the negative RSE value for the radical model *ortho-c*• confirmed the stabilization of this radical. Indeed, the odd electron is delocalized over the aromatic ring and on the oxygen atom, implying the presence of a highly stabilized mesomeric nitroxide form (E in Scheme 4 bottom), which is highlighted by the delocalization of the SOMO onto the N^+-O^- moiety (Figure 4 middle). This stabilization was in good agreement with the kinetic results ($k_{d,2c} > k_{d,2a}$ and $k_{d,2c} > k_{d,2b}$ for the major diastereoisomer). Interestingly, the NBO charge of the *ipso* carbon atom in 2c is higher than that in 3c (+0.163 vs -0.076, respectively) whereas radical model *ortho-c*• is less stabilized (RSE = -9.2 kJ/mol) than the corresponding radical model *para-c*• for 3c (RSE = -25.3 kJ/mol).¹⁴ This means that for activation at the *ortho* and *meta* positions, the trends are qualitatively the same while they differ quantitatively, although they are balanced, i.e., the larger polar effect in 2c than in 3c balances the lower stabilization for *ortho-c*• than for *para-c*•, affording very close k_d values for the major diastereoisomers of 2c and 3c.

CONCLUSION

The results reported above highlight the importance of polar and stabilization effects on the increase in the homolysis rates for alkoxyamines by activation of the pyridine moiety as well as of the effect of congestion around the pyridinyl on the activation modes, as benzylation and methylation are forbidden for 2a, in sharp contrast with 3a, and amine–borane 2g is unstable. Although the change in E_a looks small (e.g., a change of 16 kJ/mol in going from 2a to 2b), it generates dramatic changes in the half-life (e.g., a decrease from 6 months for 2a to 6 h for 2b at rt). These facts are interesting considering that chemicals such as alkoxyamines are regulated through the REACH guidelines, and their activation energy, and thus their

stability, can be tuned by chemical activation. Such opportunities open new aspects for applications in NMP and radical chemistry at low temperatures.

EXPERIMENTAL SECTION

General Information. All corresponding glassware was oven-dried (80 °C) and/or carefully dried in line with a flameless heat gun. All solvents were used as received. Routine monitoring of reactions was performed using aluminum-supported silica gel 60 F₂₅₄ TLC plates; spots were visualized using UV light and ethanolic acidic *p*-anisaldehyde solution or ethanolic phosphomolybdic solution followed by heating. Purifications by means of column chromatography were performed with silica gel 60 (230–400 mesh) and gradients of Et₂O/pentane, AcOEt/pentane, acetone/pentane, or MeOH/CH₂Cl₂. ¹H, ¹³C, and ³¹P NMR spectra were recorded in CDCl₃ or C₆D₆ solutions on 300 or 400 MHz spectrometers. Chemical shifts (δ) are reported in parts per million using residual nondeuterated solvents as internal references; min and Maj stand for minor and major diastereoisomers, respectively. High-resolution mass spectrometry (HRMS) was performed using a mass spectrometer equipped with pneumatically assisted atmospheric pressure ionization. The sample was ionized by positive-mode electrospray ionization under the following conditions: electrospray voltage (ISV), 5500 V; orifice voltage (OR), 80 V; nebulizing gas flow pressure (air), 20 psi. The mass spectra were obtained using a time-of-flight (ToF) analyzer. The measurements were realized in triplicate with double internal standardization. Each sample was dissolved in CH₂Cl₂ (400 μ L) and then diluted (dilution factor 1/10⁴) in a methanolic solution of ammonium acetate (3 mM). The sample solution was infused into the ionization source at a flow rate of 10 μ L/min.

Diethyl (1-(*tert*-Butyl(1-(pyridin-2-yl)ethoxy)amino)-2,2-dimethylpropyl)phosphonate (2a). To a stirred suspension of CuBr (1.34 g, 9.35 mmol, 0.55 equiv) and metallic Cu (1.19 g, 18.7 mmol, 1.1 equiv) in degassed benzene (40 mL) was added *N,N,N',N'',N'''*-pentamethyldiethylenetriamine (2.00 mL, 9.35 mmol, 0.55 equiv). The resulting mixture was stirred under argon at room temperature for 30 min, and then a solution of 2-(1-bromoethyl)pyridine³¹ (3.48 g, 18.7 mmol, 1.1 equiv) and SG1 (5.00 g, 17.0 mmol, 1.0 equiv) in degassed benzene (40 mL) was slowly added. The mixture was stirred under argon at room temperature for 12 h. It was then diluted with ethyl acetate, filtered, and washed several times with saturated aqueous ammonia solution, water, and brine. After drying with Na₂SO₄, filtration, and concentration in vacuo, column chromatography on silica gel gave 2a (5.93 g, 14.8 mmol, 87%) as a 2:1 mixture of diastereoisomers (NMR ratio). ¹H NMR (400 MHz, C₆D₆): δ 8.51–8.47 (m, 1H, min and Maj), 7.73 (d, J = 7.8 Hz, 1H, Maj), 7.17–7.06 (m, 1H, min and Maj, partially overlapped), 6.65–6.60 (m, 1H, min and Maj), 5.65 (q, J = 6.8 Hz, 1H, Maj), 5.42 (q, J = 6.5 Hz, 1H, min), 4.60–4.47 (m, 1H, min), 4.40–4.27 (m, 1H, min), 4.11–4.00 (m, 1H, min), 3.98–3.70 (m, 4H, Maj), 3.57–3.45 (m, 1H, Maj, partially overlapped), 3.49 (d, J = 25.9 Hz, 1H, Maj), 3.46 (d, J = 25.6 Hz, 1H, min), 1.93 (d, J = 6.8 Hz, 3H, min), 1.80 (d, J = 6.5 Hz,

3H, Maj), 1.46 (s, 9H, min), 1.36 (s, 9H, Maj), 1.24–1.21 (m, 3H, min, partially overlapped), 1.23 (s, 9H, Maj), 1.12 (t, $J = 7.3$ Hz, 3H, min), 1.03 (t, $J = 7.0$ Hz, 3H, Maj), 0.9 (t, $J = 7.0$ Hz, 3H, Maj), 0.88 (s, 9H, min). ^{13}C NMR (75 MHz, C_6D_6): δ 164.5 (min), 162.2 (Maj), 149.4 (min), 143.3 (Maj), 135.8 (Maj), 135.7 (min), 124.0 (Maj), 122.4 (Maj), 122.3 (min), 122.2 (min), 86.3 (min), 79.8 (Maj), 70.5 (d, $J = 139.2$ Hz, min and Maj), 61.9 (d, $J = 6.1$ Hz, min), 61.6 (Maj), 61.5 (d, $J = 6.6$ Hz, Maj), 61.4 (min), 59.0 (d, $J = 7.7$ Hz, Maj), 58.8 (d, $J = 7.1$ Hz, min), 36.0 (d, $J = 5.5$ Hz, min), 35.7 (d, $J = 5.0$ Hz, Maj), 31.0 (d, $J = 6.1$ Hz, Maj), 30.5 (d, $J = 6.1$ Hz, min), 28.6 (min), 28.5 (Maj), 22.8 (min), 19.7 (Maj), 16.9 (d, $J = 6.1$ Hz, min), 16.6–16.2 (m, min and Maj). ^{31}P NMR (162 MHz, C_6D_6): δ 25.6 (min), 24.6 (Maj). HRMS (ESI) m/z : calcd for $\text{C}_{20}\text{H}_{38}\text{N}_2\text{O}_4\text{P}_1$ [$\text{M} + \text{H}$] $^+$ 401.2564, found 401.2562.

2-(1-((tert-Butyl(1-(diethoxyphosphoryl)-2,2-dimethylpropyl)amino)oxy)ethyl)pyridin-1-ium 2,2,2-Trifluoroacetate (2b). Compound **2b** was prepared in situ and was not purified. For NMR analyses, compound **2b** was prepared by adding 1.0 equiv of trifluoroacetic acid to a C_6D_6 solution of compound **2a** in an NMR tube. ^1H NMR (400 MHz, C_6D_6): δ 12.67 (br s, 1H, min and Maj), 8.49–8.46 (m, 1H, min and Maj), 7.52 (d, $J = 7.8$ Hz, 1H, Maj), 7.23–7.13 (m, 2H, min, partially overlapped), 7.07–6.90 (m, 1H, Maj), 6.60–6.50 (m, 1H, min and Maj), 5.46 (q, $J = 6.5$ Hz, 1H, Maj), 5.39 (q, $J = 7.0$ Hz, 1H, min), 4.44–4.32 (m, 1H, min), 4.29–4.17 (m, 1H, min), 4.08–3.96 (m, 1H, min), 3.94–3.84 (m, 1H, min), 3.84–3.55 (m, 4H, Maj), 3.39 (d, $J = 27.1$ Hz, 1H, Maj), 3.38 (d, $J = 26.1$ Hz, 1H, min), 1.76 (d, $J = 6.8$ Hz, 3H, min), 1.53 (d, $J = 6.5$ Hz, 3H, Maj), 1.34 (s, 9H, min), 1.20 (t, $J = 7.0$ Hz, 3H, min), 1.16 (s, 9H, Maj), 1.14 (s, 9H, Maj), 1.08 (t, $J = 7.0$ Hz, 3H, min), 0.94 (t, $J = 7.0$ Hz, Maj), 0.93 (t, $J = 7.0$ Hz, Maj), 0.79 (s, 9H, min). ^{13}C NMR (75 MHz, C_6D_6): δ 161.5 (min), 160.8 (q, $J = 36.9$ Hz, min and Maj), 158.8 (Maj), 145.6 (min), 143.9 (Maj), 142.5 (Maj), 140.6 (min), 124.7 (Maj), 124.0 (min), 123.9 (min), 117.2 (q, $J = 290$ Hz, min and Maj), 83.9 (min), 78.4 (Maj), 70.3 (d, $J = 138.6$ Hz, min), 69.3 (d, $J = 139.2$ Hz, Maj), 62.4 (d, $J = 6.6$ Hz, min), 62.2 (Maj), 62.1 (d, $J = 7.2$ Hz, Maj), 61.7 (min), 60.3 (d, $J = 7.7$ Hz, Maj), 59.7 (d, $J = 7.7$ Hz, min), 35.9 (d, $J = 5.0$ Hz, min), 35.6 (d, $J = 5.0$ Hz, Maj), 30.7 (d, $J = 6.05$ Hz, Maj), 30.4 (d, $J = 6.1$ Hz, min), 28.4 (min), 28.1 (Maj), 22.4 (min), 20.6 (Maj), 16.7 (d, $J = 5.5$ Hz, min), 16.3 (d, $J = 6.1$ Hz, Maj), 16.3 (d, $J = 6.6$ Hz, min), 16.1 (d, $J = 6.6$ Hz, Maj). ^{31}P NMR (162 MHz, C_6D_6): δ 25.3 (min), 24.7 (Maj). ^{19}F NMR (376 MHz, C_6D_6): δ -75.5 (min and Maj). HRMS analysis gave the same results as for **2a**, as **2a** was readily turned into **2b** during the ionization process.

2-(1-((tert-Butyl(1-(diethoxyphosphoryl)-2,2-dimethylpropyl)amino)oxy)ethyl)pyridine N-Oxide (2c). To a stirred solution of **2a** (500 mg, 1.25 mmol, 1.0 equiv) in CH_2Cl_2 (12.5 mL) was added *m*-CPBA (70% in water, 924 mg, 3.75 mmol, 3.0 equiv). The resulting mixture was stirred at 0 °C under argon for 30 min. It was then poured into aqueous 10% Na_2SO_3 solution, extracted three times with CH_2Cl_2 , washed with aqueous saturated NaHCO_3 solution, dried, and concentrated in vacuo. After purification by column chromatography on silica gel (gradients of acetone/hexanes), compound **2c** (476 mg, 1.14 mmol, 91% yield) was obtained as a 2:1 mixture of diastereoisomers (NMR ratio). ^1H NMR (400 MHz, CDCl_3): δ 8.18–8.14 (m, 1H, min and Maj), 7.78 (dd, $J = 8.0, 2.0$ Hz, 1H, Maj), 7.53 (dd, $J = 8.0, 2.0$ Hz, 1H, min), 7.28–7.25 (m, 1H, min and Maj, partially overlapped), 7.16–7.09 (m, 1H, min and Maj), 5.86 (q, $J = 6.8$ Hz, 1H, Maj), 5.71 (q, $J = 6.5$ Hz, 1H, min), 4.35–3.82 (m, 4H, min and Maj), 3.38 (d, $J = 27.1$ Hz, 1H, Maj), 3.32 (d, $J = 26.1$ Hz, 1H, min), 1.63 (d, $J = 6.8$ Hz, 3H, min), 1.57 (d, $J = 6.5$ Hz, 3H, Maj), 1.36 (t, $J = 7.0$ Hz, 3H, min), 1.32 (t, $J = 7.0$ Hz, 3H, min), 1.26 (s, 9H, Maj), 1.21 (s, 9H, min), 1.23–1.17 (m, 6H, Maj), 1.03 (s, 9H, Maj), 0.98 (s, 9H, min). ^{13}C NMR (75 MHz, CDCl_3): δ 155.3 (min), 154.1 (Maj), 138.9 (min), 138.6 (Maj), 125.5 (min), 125.2 (Maj), 124.4 (Maj), 123.8 (min), 123.5 (min), 123.3 (Maj), 78.7 (min), 74.4 (Maj), 69.0 (d, $J = 138.7$ Hz, min), 68.7 (d, $J = 137.6$ Hz, Maj), 61.5 (Maj), 61.4 (min), 61.0 (d, $J = 6.6$ Hz, min), 60.9 (d, $J = 6.6$ Hz, Maj), 59.2 (d, $J = 7.7$ Hz, Maj), 59.0 (d, $J = 7.7$ Hz, min), 35.4 (d, $J = 5.0$ Hz, min), 35.1 (d, $J = 5.0$ Hz, Maj), 29.8 (d, $J = 5.5$ Hz, Maj), 29.4 (d, $J = 5.5$ Hz, min), 28.1 (Maj), 27.7 (min), 21.0 (min), 18.5 (Maj), 16.4 (d,

$J = 5.0$ Hz, min), 16.0 (d, $J = 5.5$ Hz, Maj), 15.9 (d, $J = 6.6$ Hz, min), 15.7 (d, $J = 6.6$ Hz, Maj). ^{31}P NMR (162 MHz, CDCl_3): δ 25.6 (min), 24.9 (Maj). HRMS (ESI) m/z : calcd for $\text{C}_{20}\text{H}_{38}\text{N}_2\text{O}_5\text{P}_1$ [$\text{M} + \text{H}$] $^+$ 417.2513, found 417.2515.

N-Acetyl-2-(1-((tert-butyl(1-(diethoxyphosphoryl)-2,2-dimethylpropyl)amino)oxy)ethyl)pyridin-1-ium Chloride (2d). Compound **2d** was prepared in situ and was not purified. For NMR analyses, compound **2d** was prepared by adding 1.0 equiv of acetyl chloride to a C_6D_6 solution of compound **2a** in an NMR tube. ^1H NMR (400 MHz, C_6D_6): δ 8.60–8.50 (m, 1H, min and Maj), 7.81 (d, $J = 8.0$ Hz, 1H, Maj), 7.28–7.03 (m, 2H, min and Maj, partially overlapped), 6.77–6.62 (m, 1H, min and Maj), 5.82 (q, $J = 6.3$ Hz, 1H, Maj), 5.58 (q, $J = 6.7$ Hz, 1H, min), 4.59–4.47 (m, 1H, min), 4.40–4.29 (m, 1H, min), 4.11–3.99 (m, 1H, min), 3.72–3.96 (m, 3H, Maj, 1H, min), 3.71–3.59 (m, 1H, Maj), 3.44 (d, $J = 25.8$ Hz, 1H, min), 3.43 (d, $J = 26.3$ Hz, 1H, Maj), 1.96 (d, $J = 6.8$ Hz, 3H, min), 1.73 (d, $J = 6.5$ Hz, 3H, Maj), 1.61 (br s, 3H, Maj), 1.53 (br s, 3H, min), 1.44 (s, 9H, min), 1.27–1.21 (m, 3H, min), 1.24 (s, 9H, Maj), 1.23 (s, 9H, Maj), 1.11 (t, $J = 7.0$ Hz, 3H, min), 1.00 (t, $J = 7.0$ Hz, 3H, Maj), 0.96 (t, $J = 7.3$ Hz, 3H, Maj), 0.86 (s, 9H, min). ^{13}C NMR (75 MHz, C_6D_6): δ 169.8 (Maj), 166.3 (min), 162.9 (min), 160.8 (Maj), 147.6 (min), 146.8 (Maj), 138.6 (Maj), 138.1 (min), 124.5 (Maj), 123.5 (Maj), 123.2 (min), 123.1 (min), 84.9 (min), 78.9 (Maj), 70.3 (d, $J = 138.7$ Hz, min), 70.0 (d, $J = 138.7$ Hz, Maj), 62.0 (d, $J = 6.1$ Hz, min), 61.8 (Maj), 61.5 (min), 61.4 (d, $J = 7.2$ Hz, Maj), 59.2 (d, $J = 7.2$ Hz, Maj), 58.9 (d, $J = 7.1$ Hz, min), 36.0 (d, $J = 5.5$ Hz, min), 35.6 (d, $J = 5.0$ Hz, Maj), 33.0 (Maj), 30.9 (d, $J = 6.1$ Hz, Maj), 30.5 (d, $J = 6.1$ Hz, min), 28.5 (min), 28.4 (Maj), 22.6 (min), 21.7 (min), 20.3 (Maj), 16.9 (d, $J = 5.5$ Hz, min), 16.6 (d, $J = 6.1$ Hz, Maj), 16.4 (d, $J = 6.6$ Hz, min), 16.3 (d, $J = 6.6$ Hz, Maj). ^{31}P NMR (162 MHz, C_6D_6): δ 25.3 (min), 24.6 (Maj). HRMS analysis could not be performed because of the instability of **2d**.

■ ASSOCIATED CONTENT

☞ Supporting Information

^1H and ^{13}C NMR spectra of **2a–d**, procedures for kinetic and pD measurements, and details of calculations of NBO charges and radical stabilization energies. This material is available free of charge via the Internet at <http://pubs.acs.org>.

■ AUTHOR INFORMATION

Corresponding Authors

*E-mail: paul.bremond@univ-amu.fr.

*E-mail: sylvain.marque@univ-amu.fr.

Notes

The authors declare no competing financial interest.

■ ACKNOWLEDGMENTS

Université d'Aix-Marseille, CNRS, and Agence Nationale de la Recherche are acknowledged for their support and an ANR grant (SonRadIs ANR-11-JS07-002-01). L.B. thanks the Agence Nationale de la Recherche for his Ph.D. grant. The authors are grateful for the time allocation for calculations from the Centre Régional de Compétence en Modélisation Moléculaire, Université d'Aix-Marseille.

■ REFERENCES

- (1) Marque, S.; Gignes, D. Nitroxide-Mediated Polymerization and its Applications. In *Encyclopedia of Radicals in Chemistry, Biology, and Materials*; Chatgililoglu, C., Studer, A., Eds.; Wiley: Chichester, U.K., 2012; pp 1813–1850 and references cited therein.
- (2) Bertin, D.; Gignes, D.; Marque, S. R. A.; Tordo, P. *Chem. Soc. Rev.* **2011**, *40*, 2189–2198.
- (3) Nicolas, J.; Guillauneuf, Y.; Lefay, C.; Bertin, D.; Gignes, D.; Charleux, B. *Prog. Polym. Sci.* **2013**, *38*, 63–235.
- (4) Grubbs, R. B. *Polym. Rev.* **2011**, *51*, 104–137.

- (5) Tebben, L.; Studer, A. *Angew. Chem., Int. Ed.* **2011**, *50*, 5034–5068.
- (6) Matyjaszewski, K. *ACS Symp. Ser.* **2012**, *1100*, 1–13.
- (7) Goto, A.; Fukuda, T. *Prog. Polym. Sci.* **2004**, *29*, 329–385.
- (8) Guillaneuf, Y.; Gimes, D.; Marque, S. R. A.; Tordo, P.; Bertin, D. *Macromol. Chem. Phys.* **2006**, *207*, 1278–1288.
- (9) Registration, Evaluation, Authorisation, and Restriction of Chemical substances (REACH), EC 1907/2006. <http://eur-lex.europa.eu/LexUriServ/LexUriServ.do?uri=CELEX:32006R1907:en:NOT> (accessed Sept 19, 2013).
- (10) Mazarin, M.; Girod, M.; Viel, S.; Phan, T. N. T.; Marque, S. R. A.; Humbel, S.; Charles, L. *Macromolecules* **2009**, *42*, 1849–1859.
- (11) Edeleva, M. V.; Kirilyuk, I. A.; Zhurko, I. F.; Parkhomenko, D. A.; Tsentalovitch, Y. P.; Bagryanskaya, E. G. *J. Org. Chem.* **2011**, *76*, 5558–5573.
- (12) Brémond, P.; Marque, S. R. A. *Chem. Commun.* **2011**, *47*, 4291–4293.
- (13) Bagryanskaya, E.; Brémond, P.; Edeleva, M.; Marque, S. R. A.; Parkhomenko, D.; Roubaud, V.; Siri, D. *Macromol. Rapid Commun.* **2012**, *33*, 152–157.
- (14) Brémond, P.; Koita, A.; Marque, S. R. A.; Pesce, V.; Roubaud, V.; Siri, D. *Org. Lett.* **2012**, *14*, 358–361.
- (15) Audran, G.; Brémond, P.; Marque, S. R. A.; Obame, G. *Polym. Chem.* **2012**, *3*, 2901–2908.
- (16) Audran, G.; Brémond, P.; Marque, S. R. A.; Obame, G. *J. Org. Chem.* **2012**, *77*, 9364–9640.
- (17) Matyjaszewski, K.; Woodworth, B. E.; Zhang, X.; Gaynor, S. G.; Metzner, Z. *Macromolecules* **1998**, *31*, 5955–5957.
- (18) Bertin, D.; Gimes, D.; Marque, S. R. A.; Tordo, P. *e-Polym.* **2003**, *2*, 1–9.
- (19) Bertin, D.; Gimes, D.; Marque, S. R. A.; Tordo, P. *Macromolecules* **2005**, *38*, 2638–2650.
- (20) One must keep in mind for the discussion that the frequency factor *A* may also be dependent on the solvent. However, for the sake of simplicity, the averaged value of *A* (see ref 19) was used.
- (21) Audran, G.; Brémond, P.; Marque, S. R. A.; Obame, G. *J. Org. Chem.* **2013**, *78*, 7754–7757.
- (22) A tentative attribution of the relative configuration of the diastereoisomers of **2a** can be done by relying on the available X-ray data for *SS/RR-3a* and on the ^1H and ^{31}P NMR data for **3a-g**, which indicate that the minor diastereoisomer of **2a** displays the *SS/RR* configuration.
- (23) As described in ref 18, samples were heated in an oil bath and then cooled in icy water, after which their ^{31}P NMR spectra were recorded at room temperature. Consequently, at 80 °C, it is likely that **2g** decomposed into **2a** and BH_3 , involving the indirect monitoring of the decay of **2a** by measuring by ^{31}P NMR spectroscopy the decay of the isomers of **2g** reformed upon cooling.
- (24) Pauling, L. *The Nature of the Chemical Bond*, 3rd ed.; Cornell University Press: Ithaca, NY, 1960; p 212.
- (25) Zavitsas, A. A. Thermochemistry and Hydrogen Transfer Kinetics. In *Encyclopedia of Radicals in Chemistry, Biology, and Materials*; Chatgililoglu, C., Studer, A., Eds.; Wiley: Chichester, U.K., 2012; pp 81–106.
- (26) Henderson, J. J. *Am. J. Physiol.* **1908**, *21*, 173–179.
- (27) Andon, R. J. L.; Cox, J. D.; Herington, E. F. G. *Trans. Faraday Soc.* **1954**, *50*, 918–927.
- (28) Beaudoin, E.; Bertin, D.; Gimes, D.; Marque, S. R. A.; Siri, D.; Tordo, P. *Eur. J. Org. Chem.* **2006**, *7*, 1555–1768.
- (29) Bertin, D.; Gimes, D.; Marque, S. R. A.; Siri, D.; Tordo, P.; Trappo, G. *ChemPhysChem* **2008**, *9*, 272–281.
- (30) For the isodesmic reaction used, see the Supporting Information.
- (31) Bull, S. D.; Davies, S. G.; Epstein, S. W.; Garner, A. C.; Mujtaba, N.; Roberts, P. M.; Savory, E. D.; Smith, A. D.; Tamayo, J. A.; Watkin, D. J. *Tetrahedron* **2006**, *62*, 7911–7925.